

QUT Digital Repository:  
<http://eprints.qut.edu.au/>



Bevrani, Hassan and Mitani, Yasunori and Tsuji, Kiichiro (2004) Robust LFC design using mixed H2/Hinf technique. In *Proceedings International Conference on Electrical Engineering (ICEE) 2004*, Sapporo, Japan.

© Copyright 2004 (please consult author)

# Robust LFC Design Using Mixed $H_2 / H_\infty$ Technique

Hassan Bevrani\*, Yasunori Mitani\*\* and Kiichiro Tsuji\*

\*Department of Electrical Eng., Osaka University, 2-1 Yamada-Oka, Suita, Osaka 565-0871, Japan

\*\*Department of Electrical Eng., Kyushu Institute of Technology, Kyushu, Japan

## Abstract

This paper addresses a new decentralized robust control design for load-frequency control (LFC) in multi-area power systems. The LFC problem is considered as a multi-objective problem and formulated via a mixed  $H_2/H_\infty$  control technique, then it is easily carried out to synthesis the desired robust controllers by solving standard linear matrix inequalities (LMI). A three-area power system example with a wide range of load changes is given to illustrate the proposed approach. The results are compared with pure  $H_\infty$  method. It is shown that the designed controllers maintain the robust performance, minimize the effect of disturbances and specified uncertainties, effectively.

*Keywords: LFC, mixed  $H_2/H_\infty$  control, power system, LMI, robust performance*

## 1 INTRODUCTION

Load-frequency control (LFC), as an ancillary service, acquires a fundamental role for maintaining the electrical system reliability at an adequate level. Naturally, LFC is a multi-objective problem. LFC goals, i.e. frequency regulation and tracking the load changes, maintaining the tie-line power interchanges to specified values in presence of generation constraints and dynamical model uncertainties determines the LFC synthesis as a multi-objective control problem. Therefore, it is expected that an appropriate multi-objective control strategy gives better solution for this problem.

However, in the reported robust LFC approaches, only one single norm is used to capture design specifications. It is clear that meeting all LFC design objectives by single control approach with regard to increasing the complexity and changing of power system structure is difficult. Furthermore each robust method is mainly useful to capture a set of special specifications. For instance, the regulation against random disturbances more naturally can be addressed by LQG or  $H_2$  synthesis. The  $H_2$  tracking design is more adapted to deal with transient performance by minimizing the linear quadratic cost of tracking error and control input, while  $H_\infty$  approach (and  $\mu$  as a generalized  $H_\infty$  approach) is more useful to holding closed-loop stability in presence of control constraints and uncertainties. While the  $H_\infty$  norm is natural for norm-bounded perturbations, in many applications the natural norm for the input-output performance is the  $H_2$  norm [1]. It is shown that using the combination of  $H_2$  and  $H_\infty$  (mixed

$H_2/H_\infty$ ) allows a better performance for a control design problem including both set of above objectives. The promise of a successful combination the methods of  $H_2$  and  $H_\infty$  control was started in the late 1980s [2].

In this paper, first the LFC problem is formulated as a multi-objective control problem for a given general control area with several generation units in a multi-area power system and then it is solved by a mixed  $H_2/H_\infty$  control approach to obtain the desired robust decentralized controller. The model uncertainty in each control area is covered by an unstructured multiplicative uncertainty block. The proposed strategy is applied to a three-control area example. Obtained results show the controllers guarantee the robust performance for a wide range of operating conditions. The results of the proposed multi-objective approach are compared with the proposed dynamic pure  $H_\infty$  controllers (using general LMI technique), which show the effectiveness of this methodology. The preliminary steps of this work are presented in [3].

## 2 PROPOSED CONTROL STRATEGY

In this paper, we use the conventional model for each control area, which is widely used in LFC literature by the researchers. Actually, power system have a highly nonlinear and time-varying nature, however a simplified and linearized model is usually used for LFC synthesis. The simplification and linearization can be considered in robust control strategies. Fig. 1 shows the block diagram of control area  $i$ , which includes  $n$  generation companies (Gencos), from an  $N$ -control area power system.

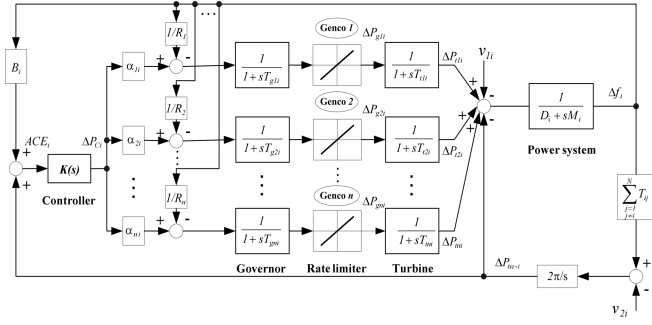


Figure 1. A general control area

Where,

$$v_{li} = \Delta P_{di} \quad (1)$$

$$v_{2i} = \sum_{\substack{j=1 \\ j \neq i}}^N T_{ij} \Delta f_j \quad (2)$$

and,

$\Delta f_i$ : frequency deviation,  $\Delta P_{gi}$ : governor valve position,  $\Delta P_{ci}$ : governor load setpoint,  $\Delta P_{ti}$ : turbine power,  $\Delta P_{tie-i}$ : net tie-line power flow,  $\Delta P_{di}$ : area load disturbance,  $M_i$ : equivalent inertia constant,  $D_i$ : equivalent damping coefficient,  $T_{gi}$ : governor time constant,  $T_{ti}$ : turbine time constant,  $T_{ij}$ : tie-line synchronizing coefficient between area I & j,  $B_i$ : frequency bias,  $R_i$ : drooping characteristic,  $\alpha$ : ACE participation factor, and,  $\Delta P_{tie-i}$ : tie-line power changes. The main control framework in order to formulate the LFC problem via a mixed  $H_2/H_\infty$  control design for a given general control area is shown in Fig. 2.

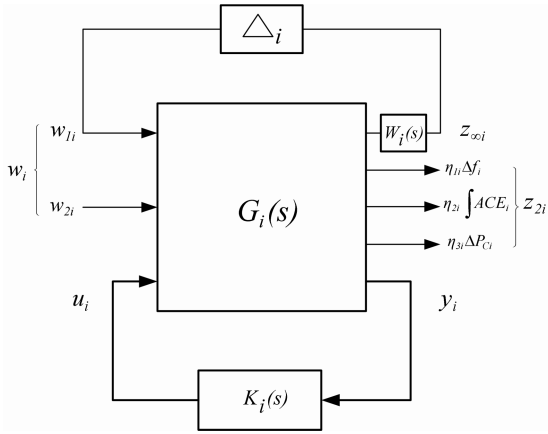


Figure 2. Mixed  $H_2/H_\infty$ -based control framework

$\Delta_i$  models the structured uncertainty set in the form of multiplicative type and  $W_i$  includes the associated weighting function. The output channels  $z_{oi}$  and  $z_{2i}$  are associated

with  $H_\infty$  and  $H_2$  (LQG aspects) performance, respectively. The  $\eta_{1i}$ ,  $\eta_{2i}$  and  $\eta_{3i}$  in Fig. 3 are constant weights that must be chosen by designer to get the desired performance, considering practical constraint on control action.  $G_i(s)$  and  $K_i(s)$  correspond to the nominal dynamical model of the given control area and controller, respectively. Also  $y_i$  is the measured output (performed by area control error ACE),  $u_i$  is control input and  $w_i$  includes the perturbed and disturbance signals in the control area.

The LFC problem as a multi-objective control problem can be expressed by the following optimization problem: design a controller that minimizes the 2-norm of the fictitious output signal  $z_{2i}$  under the constraints that the  $\infty$ -norm of the transfer function from  $w_{1i}$  to  $z_{oi}$  is less than one. On the other hand, the LFC design is reduced to find an internally stabilizing controller which minimizes  $\|T_{z_{2i} w_{2i}}\|_2$  while maintaining  $\|T_{z_{oi} w_{1i}}\|_\infty < 1$ . This problem can be solved by convex optimization using linear matrix inequalities [4].

Considering Fig. 1 and according to the proposed control framework (Fig. 2), the state space model for control area i,  $G_i(s)$ , can be obtained as follows.

$$\begin{aligned} \dot{x}_i &= A_i x_i + B_{1i} w_i + B_{2i} u_i \\ z_{oi} &= C_{oi} x_i + D_{oi} w_i + D_{oi2} u_i \\ z_{2i} &= C_{2i} x_i + D_{21i} w_i + D_{22i} u_i \\ y_i &= C_{yi} x_i + D_{yi} w_i \end{aligned} \quad (3)$$

where,

$$\begin{aligned} x_i^T &= [\Delta f_i \quad \Delta P_{tie-i} \quad \int ACE_i \quad x_{ti} \quad x_{gi}] \\ x_{ti} &= [\Delta P_{t1i} \quad \Delta P_{t2i} \quad \dots \quad \Delta P_{tmi}]^T, \quad x_{gi} = [\Delta P_{g1i} \quad \Delta P_{g2i} \quad \dots \quad \Delta P_{gni}]^T \\ u_i &= \Delta P_{Ci}, \quad w_i^T = [w_{1i} \quad w_{2i}]^T, \quad w_{2i}^T = [v_{1i} \quad v_{2i}]^T \\ z_{2i}^T &= [\eta_{1i} \Delta f_i \quad \eta_{2i} \int ACE_i \quad \eta_{3i} \Delta P_{Ci}]^T \end{aligned}$$

and,

$$A_i = \begin{bmatrix} A_{i11} & A_{i12} & A_{i13} \\ A_{i21} & A_{i22} & A_{i23} \\ A_{i31} & A_{i32} & A_{i33} \end{bmatrix}, \quad B_{1i} = \begin{bmatrix} B_{1i1} \\ B_{1i2} \\ B_{1i3} \end{bmatrix}, \quad B_{2i} = \begin{bmatrix} B_{2i1} \\ B_{2i2} \\ B_{2i3} \end{bmatrix}$$

$$A_{i11} = \begin{bmatrix} -D_i/M_i & -1/M_i & 0 \\ 2\pi \sum_{\substack{j=1 \\ j \neq i}}^N T_{ij} & 0 & 0 \\ B_i & 1 & 0 \end{bmatrix}, \quad A_{i12} = \begin{bmatrix} 1/M_i & \dots & 1/M_i \\ 0 & \dots & 0 \\ 0 & \dots & 0 \end{bmatrix}_{3 \times n}$$

$$A_{i22} = -A_{i23} = \text{diag}[-1/T_{t1i} \quad -1/T_{t2i} \quad \dots \quad -1/T_{tmi}]$$

$$A_{i33} = \text{diag}[-1/T_{g1i} \quad -1/T_{g2i} \quad \dots \quad -1/T_{gni}]$$

$$A_{i31} = \begin{bmatrix} -1/(T_{g1i} R_{1i}) & 0 & 0 \\ \vdots & \vdots & \vdots \\ -1/(T_{gni} R_{ni}) & 0 & 0 \end{bmatrix}, \quad A_{i13} = A_{i21}^T = 0_{3 \times n}, \quad A_{i32} = 0_{n \times n}$$

$$\begin{aligned}
B_{1i1} &= \begin{bmatrix} 0 & -1/M_i & 0 \\ 0 & 0 & -2\pi \\ 0 & 0 & 0 \end{bmatrix}, \quad B_{1i2} = 0_{n \times 3}, \quad B_{1i3} = \begin{bmatrix} \alpha_{1i}/T_{g1i} & 0 & 0 \\ \vdots & \vdots & \vdots \\ \alpha_{ni}/T_{gni} & 0 & 0 \end{bmatrix} \\
B_{2i1} &= 0_{3 \times 1}, \quad B_{2i2} = 0_{n \times 1}, \quad B_{2i3}^T = [\alpha_{1i}/T_{g1i} \quad \alpha_{2i}/T_{g2i} \quad \cdots \quad \alpha_{ni}/T_{gni}] \\
C_{\infty i} &= 0_{1 \times (2n+3)}, \quad D_{\infty 1i} = \begin{bmatrix} -1 & 0 & 0 \end{bmatrix}, \quad D_{\infty 2i} = 1 \\
C_{2i} &= [c_{2i1} \quad c_{2i2}], \quad c_{2i1} = \begin{bmatrix} \eta_{1i} & 0 & 0 \\ 0 & 0 & \eta_{2i} \\ 0 & 0 & 0 \end{bmatrix}, \quad c_{2i2} = 0_{3 \times 2n} \\
D_{2i1} &= 0_{3 \times 3}, \quad D_{2i2} = \begin{bmatrix} 0 \\ 0 \\ \eta_{3i} \end{bmatrix} \\
C_{yi} &= [c_{yi} \quad 0_{2 \times 2n}], \quad c_{yi} = \begin{bmatrix} \beta_i & 1 & 0 \\ 0 & 0 & 1 \end{bmatrix}, \quad D_{yi} = 0_{2 \times 3}
\end{aligned}$$

The proposed control framework shown in Fig. 2, covers all mentioned LFC objectives. The  $H_2$  performance is used to minimize the effects of disturbances on area frequency and area control error (ACE) by introducing fictitious controlled outputs  $\eta_{1i}\Delta f_i$  and  $\eta_{2i}\int ACE_i$ . In result, the tie-line power flow which can be described as a linear combination of frequency deviation and ACE signals,

$$\Delta P_{tie-i} = ACE_i - B_i \Delta f_i \quad (4)$$

is controlled. Furthermore fictitious output  $\eta_{3i}\Delta P_{Ci}$  sets a limit on the allowed control signal to penalize fast changes and large overshoot in the governor load set-point with regards to corresponded practical constraint on power generation by generator units. Also in LFC, it is important to keep up the frequency regulation and desired performance in the face of uncertainties affecting the control area [5]. The  $H_\infty$  performance is used to meet the robustness against specified uncertainties and reduction of its impact on closed-loop system performance. Therefore, it is expected that the proposed strategy satisfy the main objectives of LFC system under load disturbance and model uncertainties.

In the next section, two sets of robust controllers are developed for a power system example including three control areas. The first one includes pure  $H_\infty$  controllers based on general LMI technique and the second one contains designed reduced-order controllers based on the proposed mixed  $H_2/H_\infty$  approach with the assumed same objectives and initializations to achieve desired robust performance.

### 3 CASE STUDY

To illustrate the effectiveness of proposed control strategy, a three control area power system, shown in Fig. 3, is considered as a test system. It is assumed that each control area includes three Gencos. The power system parameters are considered the same as [6].

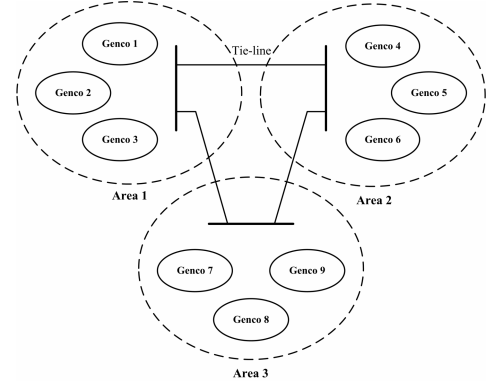


Figure 3. Three control area power system

### 3.1. Uncertainty And Performance Weights Selection

In this example with regards to uncertainty, it is assumed that the parameters of rotating mass and load pattern in each control area have uncertain values. The variation range for  $D_i$  and  $M_i$  parameters in each control area is assumed  $\pm 20\%$ . Following, we will model these uncertainties as an unstructured multiplicative uncertainty block that contains all the information available about  $D_i$  and  $M_i$  variations.

Corresponding to an uncertain parameter, let  $\hat{G}_i(s)$  denotes the transfer function from the control input  $u_i$  to control output  $y_i$  at operating points other than nominal point. Following a practice common in robust control, we will represent this transfer function as

$$\hat{G}_i(s) = G_i(s)(I + \Delta_i(s)W_i(s)) \quad (5)$$

$\Delta_i(s)$  shows the uncertainty block corresponding to uncertain parameter,  $W_i(s)$  is the associated weighting function and  $G_i(s)$  is the nominal transfer function model. Then the multiplicative uncertainty block can be expressed as

$$|\Delta_i(s)W_i(s)| = \left| \frac{\hat{G}_i(s) - G_i(s)}{G_i(s)} \right|; \quad G_i(s) \neq 0 \quad (6)$$

where,  $\|\Delta_i(s)\|_\infty = \sup_\omega |\Delta_i(s)| \leq 1$ .

Thus,  $W_i(s)$  is such that its respective magnitude bode plot covers the bode plot of all possible plants. For example, using (6) some sample uncertainties corresponding to different values of  $D_i$  and  $M_i$  for area 1 are shown in Fig. 4. It can be seen the frequency responses of both set of parametric uncertainties are close to each other, and, hence to keep the complexity of obtained controller low, we can model uncertainties due to both set of parameters variation by using a norm bonded multiplicative uncertainty to cover all possible plants as follows

$$W_1(s) = \frac{0.2519s^2 + 0.9880s + 1.3004}{s^2 + 1.5090s + 8.3679}$$

Using the same method, the uncertainty weighting functions for areas 2 and 3 will be obtained.

$$W_2(s) = \frac{0.2384s^2 + 4.0542s + 2.0462}{s^2 + 5.3374s + 15.3922}$$

$$W_3(s) = \frac{0.2691s^2 + 0.5396s + 1.5978}{s^2 + 0.6471s + 10.4219}$$

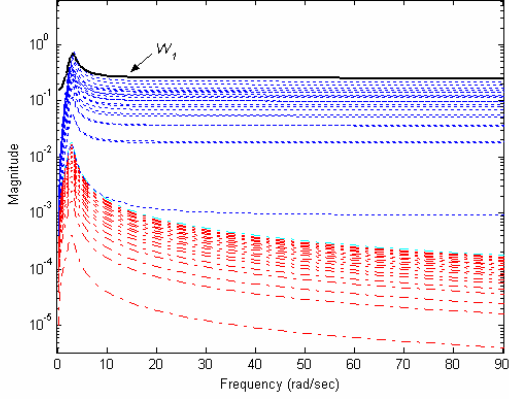


Figure 4. Uncertainty plots due to parameters changes in area 1;  $D_i$  (dotted),  $M_i$  (dash-dotted) and  $W_i$  (solid).

The selection of constant weights  $\eta_{1i}$ ,  $\eta_{2i}$  and  $\eta_{3i}$  is dependent on specified performance objectives and must be chosen by designer. In fact an important issue with regard to selection of these weights is the degree to which they can guarantee the satisfaction of design performance objectives. The selection of these weights entails a trade off among several performance requirements. The coefficients  $\eta_{1i}$  and  $\eta_{2i}$  at controlled outputs set the performance goals e.t. tracking the load variation and disturbance attenuation.  $\eta_{3i}$  sets a limit on the allowed control signal to penalize fast change and large overshoot in the governor load set-point signal. Here, a set of suitable values for constant weights is chosen as follows:

$$\eta_{1i} = 0.20, \quad \eta_{2i} = 1.30, \quad \eta_{3i} = 1.75$$

### 3.2. Resulted Controllers

At the next step, according to synthesis methodology (mixed  $H_2/H_\infty$ ) described in section 2, a set of three decentralized robust controllers are designed. Specifically, the control design is reduced to an LMI formulation, and then the multi-objective control problem is solved according to existing LMI constraints. The order of resulting controllers is 11 (almost it is equal to the size of area model plus  $W_i(s)$ ). Using the standard Hankel norm approximation, the order of  $K_1(s)$ ,  $K_2(s)$  and  $K_3(s)$  are reduced to 3, 4 and 6 respectively, with no performance degradation. The reduced-order controllers are given in the appendix. The optimal performance indices for the original and reduced order controllers are listed in table 1.

Table 1. Robust performance index

Performance index	Area 1	Area 2	Area 3
$\gamma_2$ (Original)	3.610	3.230	3.240
$\gamma_\infty$ (Original)	0.966	0.960	0.982
$\gamma_2$ (Reduced)	3.650	3.290	3.270
$\gamma_\infty$ (Reduced)	0.975	0.963	0.996

In order to comparison, for each control area, in addition to proposed control strategy, a pure  $H_\infty$  dynamic output controller is developed using the function *hinflmi*, provided by the MATLAB's LMI control toolbox [4] to achieve the same objectives. The LFC design using this method (LMI-based  $H_\infty$ ) is already reported in [6].

## 4 SIMULATION RESULTS

In order to demonstrate the effectiveness of the proposed strategy, some simulations were carried out. In these simulations, the proposed reduced-order controllers were applied to the three control area power system described in Fig. 3. The results are compared with full-order pure  $H_\infty$  controllers for the various scenarios of load disturbances and uncertainties.

**Scenario 1:** As the first test case, the power system is considered without uncertainties and it is assumed a large step load disturbance 0.1 pu is applied to each control area at 2s. Frequency deviation, control action signals and area control error of closed-loop system are shown in Figs. 5 and 6. Comparing the simulation results with both types of controllers, in Fig. 5, shows that the proposed design achieves better frequency regulation with small settling times. Using the proposed method, the area control error and frequency deviation of all areas are quickly driven back to zero.

**Scenario 2:** In this scenario, the closed-loop performance is tested in presence of both disturbance and uncertainties. It is assumed that in addition to applying a step load disturbance 0.1 pu, the simulation is done following %20 decrease in uncertain parameters  $D_i$  and  $M_i$ . The frequency deviation and control action signals of the closed-loop system are shown in Figs. 7.

**Scenario 3:** As an other sever condition, assume in addition to %20 increase in  $D_i$  and  $M_i$ , a bounded random load change (shown in Fig. 8) is applied to each control area, where

$$-0.05 \text{ pu} \leq \Delta P_{di} \leq +0.05 \text{ pu}$$

The purpose is to test the robustness of the proposed controllers against uncertainties and random load disturbances. The closed-loop response for area 1 and 3 are shown in Fig. 9. It is seen that proposed design give small frequency deviation amplitude using less control effort with smooth changes, which is more useful in real-world LFC applications. These figures demonstrate that the designed controllers track the load fluctuations and meet robustness, effectively.

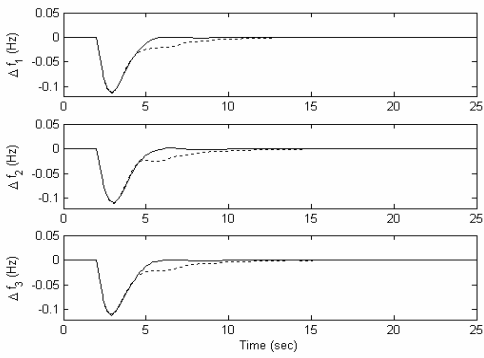
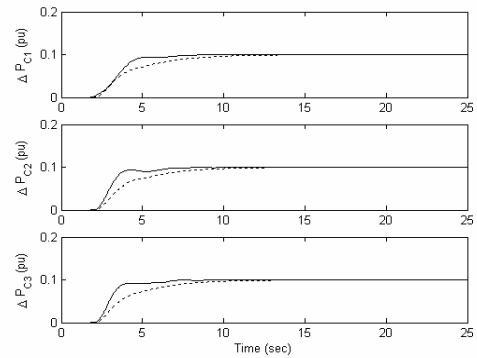
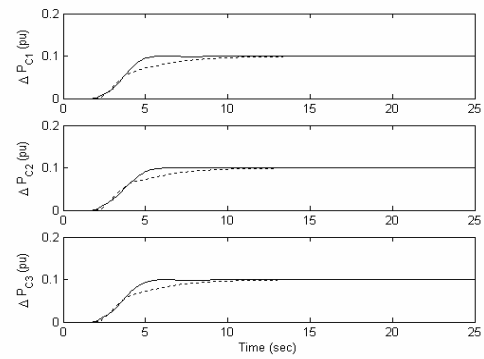


Figure 5. Frequency deviation; solid ( $H_2/H_\infty$ ), dotted ( $H_\infty$ ).

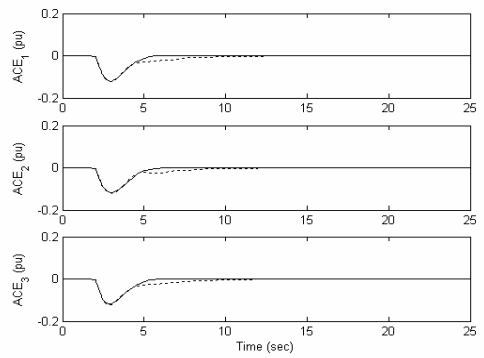


(b)

Figure 7. (a) Frequency deviations, (b) Control action signals for scenario 2; solid ( $H_2/H_\infty$ ), dotted ( $H_\infty$ ).

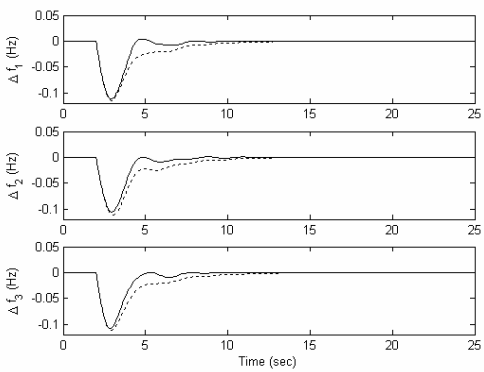


(a)



(b)

Figure 6. (a) Control action response, (b) Area control error for scenario 1; solid ( $H_2/H_\infty$ ), dotted ( $H_\infty$ ).



(a)

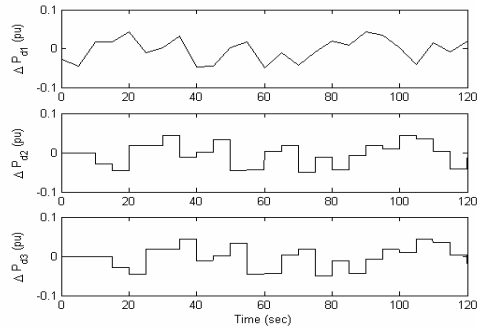
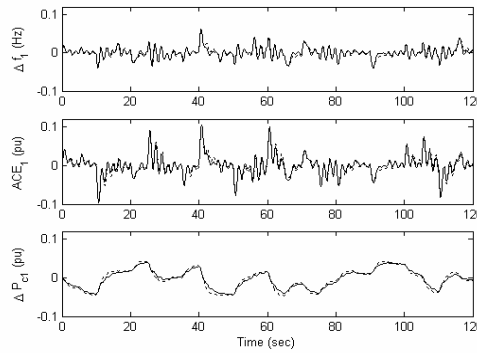
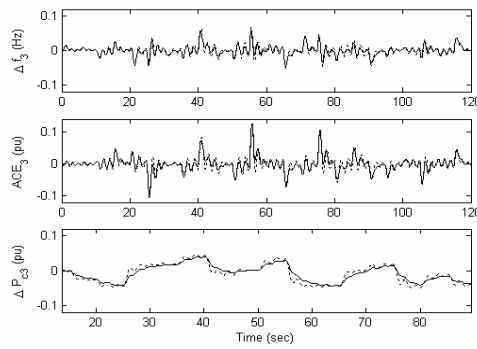


Figure 8. Random load patterns



(a)



(b)

Figure 9. The closed-loop response in: (a) area 1 and (b) area 3 for scenario 3; solid ( $H_2/H_\infty$ ), dotted ( $H_\infty$ ).

## 5 CONCLUSION

Since in real-world power system, each control area is faced with various uncertainties and disturbances, the LFC problem in a multi-area power system is formulated as a decentralized multi-objective optimization control problem. A mixed  $H_2/H_\infty$  technique is used to solve it and design the desired controllers.

The proposed method was applied to a three control area power system and is tested under various possible scenarios. The results are compared with the results of applied dynamic output  $H_\infty$  controllers. It was shown that the designed controllers are capable to guarantee the robust performance such as precise reference, frequency tracking and disturbance attenuation under a wide range of area-load disturbances and specified uncertainties.

## REFERENCES

- [1] K. Zhou, K. Glover, B. Bodenheimer, J. Doyle, "Mixed  $H_2$  and  $H_\infty$  performance objectives I: Robust performance analysis," IEEE Trans. Automat. Control, vol. 39, no. 8, pp. 1564-1574, 1994.
- [2] DS. Bernstein, WM. Haddad, "LQG control with  $H_\infty$  performance bound," IEEE Trans. Automat. Control, vol. 34, no. 3, pp. 293-305, 1989.
- [3] H. Bevrani, Y. Mitani, K. Tsuji, "Robust decentralized AGC in a restructured power system," Accepted to publish in Energy Conversion & Management, 2004.
- [4] P. Gahinet, A. Nemirovski, A. J. Laub, M. Chilali, "LMI Control Toolbox," The MathWorks, Inc., 1995.
- [5] H. Bevrani, Y. Mitani, K. Tsuji, "On robust load-frequency regulation in a restructured power system," IEEJ Trans. on Power and Energy, vol. 124, no. 2, pp. 190-198, 2004
- [6] D. Rerkpreedapong, A. Hasanovic, A. Feliachi, "Robust load frequency control using genetic algorithms and linear matrix inequalities," IEEE Trans. Power Systems, vol. 18, no. 2, pp. 855-861, 2003.

## APPENDIX

Designed load frequency controllers:

$$\begin{aligned}\dot{x}_{ki} &= A_{ki}x_{ki} + B_{ki}y_i \\ u_i &= C_{ki}x_{ki} + D_{ki}y_i\end{aligned}$$

where,

$$\begin{aligned}A_{kl} &= \begin{bmatrix} -2.84 & -1.82 & -0.45 \\ 1.55 & -1.30 & -0.71 \\ 0.27 & -0.67 & -1.95 \end{bmatrix}, B_{kl} = \begin{bmatrix} -0.35 & 1.21 \\ -0.28 & -0.21 \\ -0.093 & -0.034 \end{bmatrix} \\ C_{kl}^T &= \begin{bmatrix} -1.26 \\ -0.35 \\ -0.1 \end{bmatrix}, D_{kl}^T = \begin{bmatrix} -0.16 \\ -0.03 \end{bmatrix} \\ A_{k2} &= \begin{bmatrix} -7.84 & -43.5 & 3.46 & -0.90 \\ 43.47 & -53.48 & 11.62 & -3.76 \\ -3.43 & 11.25 & -5.37 & 3.13 \\ -0.89 & 3.74 & -3.00 & -9.17 \end{bmatrix}\end{aligned}$$

$$\begin{aligned}C_{k2}^T &= \begin{bmatrix} 36.10 \\ 59.85 \\ -7.48 \\ 2.09 \end{bmatrix}, D_{k2}^T = \begin{bmatrix} 0.024 \\ -90.26 \end{bmatrix}, B_{k2} = \begin{bmatrix} 1.77 & 36.06 \\ 0.66 & -59.85 \\ 1.53 & 7.33 \\ -0.20 & 2.08 \end{bmatrix} \\ A_{k3} &= \begin{bmatrix} -2.28 & 24.08 & 1.70 & 0.17 & 0.17 & 0.49 \\ -24.04 & -17.65 & -5.17 & -0.62 & -0.65 & -1.78 \\ -1.68 & -4.96 & -4.17 & -0.10 & -1.06 & -2.67 \\ 0.017 & 0.61 & 1.02 & -0.37 & -3.72 & -1.73 \\ 0.017 & 0.63 & 0.96 & 2.98 & -0.41 & -1.82 \\ 0.05 & 1.78 & 2.56 & -1.66 & -1.77 & -12.64 \end{bmatrix} \\ B_{k3} &= \begin{bmatrix} 2.54 & 25.38 \\ -0.98 & 54.63 \\ 2.09 & 8.61 \\ -0.17 & -0.93 \\ 0.23 & -0.96 \\ -0.14 & -2.74 \end{bmatrix}, C_{k3}^T = \begin{bmatrix} 25.51 \\ -54.63 \\ -8.86 \\ -0.95 \\ -1.00 \\ -2.75 \end{bmatrix}, D_{k3}^T = \begin{bmatrix} -0.03 \\ -98.71 \end{bmatrix}\end{aligned}$$

## BIOGRAPHIES

**Hassan Bevrani** received his M.Sc. degree (first class honors) in Electrical Engineering from K. N. Toosi University of Technology, Tehran, Iran in 1997. He is currently a Ph.D student at Osaka University, Japan. His special fields of interest included robust control and modern control applications in Power system and Power electronic industry. He is an academic member at Kurdistan University (Iran) and a member of the Institute of Electrical Engineers of Japan, IEE, and IEEE.

**Yasunori Mitani** received his B.Sc., M.Sc., and Dr. of Engineering degrees in electrical engineering from Osaka University, Japan in 1981, 1983, and 1986 respectively. He joined the Department of Electrical Engineering of the same university in 1990. He is currently a professor in Kyushu Institute of Technology. His research interests are in the areas of analysis and control of power systems. He is a member of the Institute of Electrical Engineers of Japan, the Institute of Systems, Control and Information Engineers of Japan, and the IEEE.

**Kiichiro Tsuji** received his B.Sc and M.Sc. degrees in electrical engineering from Osaka University, Japan, in 1966 and 1968, respectively, and his Ph.D in systems engineering from Case Western Reserve University, Cleveland, Ohio in 1973. In 1973 he joined the Department of Electrical Engineering, Osaka University, and is currently a professor at Osaka University. His research interests are in the areas of analysis, planning, and evaluation of energy systems, including electrical power systems. He is a member of the Institute of Electrical Engineers of Japan, the Japan Society of Energy and Resources, the Society of Instrument and Control Engineers, the Institute of Systems, Control and Information Engineers, and the IEEE.